Frontiers in Bioscience Landmark

Front. Biosci. (Landmark Ed) **2024**; 29(8): 303
https://doi.org/10.31083/j.fbl2908303

Original Research

Inhibition of Macrophage Recruitment to Heart Valves Mediated by the C-C Chemokine Receptor Type 2 Attenuates Valvular Inflammation Induced by Group A Streptococcus in Lewis Rats

Ling Bai[1,2,3,†], Yuan Li[1,2,3,†], Yan Xue[1,2,3,†], Zirong Lu[1,2,3], Zhongyuan Meng[1,2,3], Chuanghong Lu[1,2,3], Feng Huang[1,2,3,*], Zhiyu Zeng[1,2,3,*]

[1]Department of Cardiology, The First Affiliated Hospital of Guangxi Medical University, 530021 Nanning, Guangxi, China
[2]Guangxi Key Laboratory of Precision Medicine in Cardio-cerebrovascular Diseases Control and Prevention, 530021 Nanning, Guangxi, China
[3]Guangxi Clinical Research Center for Cardio-Cerebrovascular Diseases, 530021 Nanning, Guangxi, China
*Correspondence: huangfeng@stu.gxmu.edu.cn (Feng Huang); zengzhiyu@gxmu.edu.cn (Zhiyu Zeng)
[†]These authors contributed equally.

Academic Editor: Rajesh Katare
Submitted: 17 May 2024 Revised: 11 July 2024 Accepted: 16 July 2024 Published: 22 August 2024

Abstract

Background: Rheumatic heart disease (RHD) is an autoimmune disease caused by recurrent infections of Group A streptococcus (GAS), ultimately leading to inflammation and the fibrosis of heart valves. Recent studies have highlighted the crucial role of C-C chemokine receptor type 2-positive ($CCR2^+$) macrophages in autoimmune diseases and tissue fibrosis. However, the specific involvement of $CCR2^+$ macrophages in RHD remains unclear. **Methods**: This study established an RHD rat model using inactivated GAS and complete Freund's adjuvant, demonstrating a correlation between $CCR2^+$ macrophages and fibrosis in the mitral valves of these rats. **Results**: Intraperitoneal injection of the CCR2 antagonist Rs-504393 significantly reduced macrophage infiltration, inflammation, and fibrosis in valve tissues of RHD rats compared to the solvent-treated group . Existing evidence suggests that C-C motif chemokine ligand 2 (CCL2) acts as the primary recruiting factor for $CCR2^+$ cells. To validate this, human monocytic leukemia cells (THP-1) were cultured *in vitro* to assess the impact of recombinant CCL2 protein on macrophages. CCL2 exhibited pro-inflammatory effects similar to lipopolysaccharide (LPS), promoting M1 polarization in macrophages. Moreover, the combined effect of LPS and CCL2 was more potent than either alone. Knocking down *CCR2* expression in THP-1 cells using small interfering RNA suppressed the pro-inflammatory response and M1 polarization induced by CCL2. **Conclusions**: The findings from this study indicate that $CCR2^+$ macrophages are pivotal in the valvular remodeling process of RHD. Targeting the CCL2/CCR2 signaling pathway may therefore represent a promising therapeutic strategy to alleviate valve fibrosis in RHD.

Keywords: rheumatic heart disease; macrophage; fibrosis; CCR2 antagonist

1. Introduction

Rheumatic heart disease (RHD) is a leading cause of cardiac mortality in adolescents and remains a significant global public health challenge [1]. Acute rheumatic fever (ARF) typically manifests approximately three weeks after a pharyngeal infection with Group A streptococcus (GAS), with RHD representing its most severe complication [2]. Pathological changes in RHD arise from recurrent asymptomatic ARF episodes, leading to cumulative chronic damage to the heart valves. This process ultimately results in regurgitation and/or stenosis of the mitral and/or aortic valves, precipitating complications [3]. However, understanding of the drivers and specific biological processes underlying inflammation and fibrosis development in RHD valves remains limited.

A substantial body of research on RHD supports the perspective that immune cells and the cytokines they produce act as mediators of valve damage [4,5]. Studies on immune cells have shown widespread infiltration of $CD4^+$ T cells in RHD valves. These $CD4^+$ T cells not only recognize the pathogenic M protein of streptococci but also target self-antigens in cardiac tissues, resulting in secretion of various cytokines [6,7]. Recent experimental evidence has uncovered the crucial role of macrophages in regulating inflammation and fibrosis within RHD valves [8,9]. Notably, depleting macrophages alleviates valve inflammation, highlighting their potential role in valve myocarditis [10]. The C-C chemokine receptor type 2 (CCR2) receptor is primarily expressed on the surface of monocytes and macrophages and is considered to play a critical role in guiding macrophage infiltration into sites of inflammation [11]. The interaction between the CCR2 and C-C motif chemokine ligand 2 (CCL2) receptors has been extensively validated, emphasizing their significant involvement in the pathogenesis of various autoimmune diseases such as rheumatoid arthritis, osteoarthritis, lupus nephritis, and scleroderma [12–15]. Furthermore, these receptors are closely associated with processes such as cardiac fibrosis, liver fibrosis, renal fibrosis, and cystic fibro-

sis [16–20]. Therefore, investigating the potential role of the CCL2/CCR2 axis in mediating macrophage recruitment and activation is crucial for understanding the remodeling of RHD valves.

This study investigated several pivotal questions: (1) Are $CCR2^+$ macrophages present in the valves of patients with RHD? (2) Is CCL2 expressed in the valve cells of RHD patients? The objective was to use an animal model to determine whether activation of the CCL2/CCR2 axis during RHD facilitates the recruitment of macrophages. (3) Does blocking the CCL2/CCR2 signaling pathway result in inhibition of macrophage recruitment and infiltration, and subsequently mitigate inflammation and fibrosis in RHD valves? (4) The role of the CCL2 protein in macrophages was also investigated *in vitro*. The study confirmed the pivotal role of $CCR2^+$ macrophages in the fibrosis process in RHD valves. This finding underscoresthe potential effectiveness of inhibiting the CCL2/CCR2 signaling pathway in macrophages as a therapeutic strategy for reducing fibrosis in the valves of patients with RHD.

2. Materials and Methods

2.1 Collection of Mitral Valve Tissue

Ethical approval for the study was obtained from the Medical Ethics Committee of the First Affiliated Hospital of Guangxi Medical University, and informed consent forms were signed by all patients and their families. Heart valves were obtained from three female patients aged 45–55 years diagnosed with RHD, who had undergone mitral valve replacement at the First Affiliated Hospital of Guangxi Medical University. Immediately after dissection, the valves were placed in pre-cooled phosphate-buffered saline, cleansed of surface blood, and then fixed in 4% paraformaldehyde (P1110, Beijing Solarbio Science & Technology Co., Ltd., Beijing, China).

2.2 Preparation of Antigen

Group A Streptococcus (GAS, American Type Culture Collection) was inoculated into Brain Heart Infusion Powder (Guangdong Huankai Microbial Technology Co., Ltd., Guangdong, China) and then incubated at 37 °C for 24 h using a rotary mixer (Fuma, Shanghai, China) at 110 r/min. Bacterial fluids were collected and fixed in 4% paraformaldehyde for 12 h, then washed five times with saline before being finally diluted to 10×10^{11} CFU/mL in saline. Antigen A was prepared by emulsification using a sonicator (Sonics & Materials, Inc, Newtown, CT, USA) at the time of administration, while antigen B was prepared by mixing 1:1 with complete Freund's adjuvant (F5881, Sigma-Aldrich, Darmstadt, Germany).

2.3 Animal Models

All animal experimental procedures adhered to ethical guidelines for animal care and use, approved by the First Affiliated Medical Ethics Committee of Guangxi Medical University Affiliated Hospital (Approval Number: 2023-E751-01). Twenty-four 10-week-old female Lewis rats were obtained from Beijing Viton Lihua Laboratory Animal Technology Co., Ltd. (Beijing, China) and were randomly assigned to three groups: Control, RHD, or RHD+Rs-504393 groups, each comprising eight rats. After one week of acclimatization and feeding in the Guangxi Medical University Laboratory Animal Center (SPF grade), the rats received an initial injection of 0.2 mL of antigen B (bacterial emulsion: complete Fuchs' adjuvant = 1:1) into the footpad under 2% concentration of isoflurane. Following a week of rest, 0.5 mL of antigen B was injected subcutaneously into the abdominal wall, repeated once a week for four consecutive weeks. Additionally, 0.5 mL of antigen A (inactivated GSA) was injected subcutaneously into the abdominal wall after a one-week rest period following the completion of the antigen B injections [21,22]. The Rs-504393 treatment group received intraperitoneal injections of 5 mg/kg of the CCR2 antagonist (Rs-504393, BD218736, Shanghai Bide Pharmaceutical Technology Co., Ltd., Shanghai, China) concurrently with the first subcutaneous injection of antigen B into the abdominal wall. This treatment was administered once daily for eight weeks. In the control group, complete Fuchs' adjuvant was injected instead of antigen B, while physiological saline was administered in place of antigen A, in equivalent amounts and at the same sites. Upon completion of all the interventions, 1 ml of blood was collected from the tail vein. Subsequently, all rats were euthanized using intraperitoneal administration of pentobarbital sodium at a concentration of 150 mg/kg to collect the heart valves.

2.4 Histology and Immunohistochemistry

The collected valve tissues were fixed in 4% paraformaldehyde for 24 h, followed by embedding in paraffin, sectioning into 4 µm thick slices, and mounting onto slides. Hematoxylin and eosin (H&E) staining was employed to evaluate inflammation, while Sirius red staining was used to assess valve fibrosis. Imaging of the H&E-stained samples was conducted using a BX43 light microscope (Olympus Corporation, Tokyo, Japan) at a magnification of ×400, and images of the Sirius red staining samples were captured using a BX43 confocal microscope (Olympus Corporation, Tokyo, Japan) at the same magnification. For immunohistochemical staining, the valve sections were incubated with CCL2 (1:200, ab25124, Abcam, Cambridge, UK), collagen-1 (COL-1, 1:500, ab316222, Abcam), CD68 (1:200, GB113109, Servicebio, Wuhan, China), CCR2 (1:200, GB11326, Servicebio), iNOS (1:200, GB11119, Servicebio), or CD206 (1:500, GB113497, Servicebio). Add the secondary antibody Goat Anti-Rabbit IgG H&L (HRP) (1:500, ab97051, Abcam) and incubate for 30 min.

2.5 Reverse Transcription Quantitative Polymerase Chain Reaction

Total RNA was extracted from both valve tissues and cells using TRIzol® reagent (15596026CN, Thermo Fisher Scientific, Inc., Waltham, MA, USA), following the manufacturer's guidelines. The cDNA first-strand synthesis kit (YFXM0009, Nanjing Yifeixue Biotechnology Co., Ltd., Nanjing, China) was then employed to reverse-transcribe the total RNA into cDNA, according to the manufacturer's protocol. Subsequently, real time-quantitative polymerase chain reaction (RT-qPCR) was performed using 2× SYBR Green qPCR Master Mix (YFXM0001, Nanjing Yifeixue Biotechnology Co., Ltd., Nanjing, China). Using the $2^{-\Delta\Delta Ct}$ method, the results were normalized to the relative expression of each target gene, with glyceraldehyde-3-phosphate dehydrogenase (*GAPDH*) or β-*actin* as reference genes. Table 1 summarized the primer sequences used in this study.

2.6 Protein Imprinting Analysis

Valve tissues or cells were lysed in RIPA buffer (R0010, Beijing Solarbio Science & Technology Co., Ltd., Beijing, China), and individual samples (30 mg of protein) were then prepared for electrophoresis on 7.5–15% sodium dodecyl sulfate (SDS)/polyacrylamide gel electrophoresis (PAGE) gels, followed by transfer to polyvinylidene fluoride (PVDF) membranes (ISEQ00005, EMD Millipore, Darmstadt, Germany). The membranes were blocked with 5% skimmed milk in TBST (T1082, Beijing Solarbio Science & Technology Co., Ltd, Beijing, China) for 1 h at room temperature, washed three times, and subsequently incubated at 4 °C overnight with the following specific primary antibodies: anti-CCR2 (1:1000, ab223366, Abcam, Cambridge, UK), anti-CCR2 (1:1000, 16153-1-AP, Proteintech, Wuhan, China), anti-CCL2 (1:2000, ab25124, Abcam), anti-α-smooth muscle actin (α-SMA) (1:10,000, ab124964, Abcam), anti-COL1A1 (1:1000, ab316222, Abcam), anti-COL3A1 (1:1000, ab184993, Abcam), anti-CD86 (1:1000, CY5238, Abways, Beijing, China), anti-GAPDH (1:10,000, ab181602, Abcam), and Tubulin (1:5000, 11224-1-AP, Proteintech). After washing, the membranes were incubated for 1 h with an HRP-coupled secondary antibody (1:10,000, ab97051, Abcam). The final bands were visualized using an ECL chemiluminescence kit (P2200, Suzhou New Saimei Biotechnology Co., Ltd., Suzhou, China). Quantify the grayscale values of the bands corresponding to the final target protein using Image J software 1.53t (National Institutes of Health, Bethesda, MD, USA).

2.7 Immunofluorescence Staining

Tissue samples were rapidly frozen in liquid nitrogen and processed using the indirect immunofluorescence technique. Frozen sections were stained overnight at 4 °C in a humidified room with primary antibodies targeting anti-CD68 (1:2000, GB113109, Servicebio, Wuhan, China), anti-CCR2 (1:200, GB11326, Servicebio), anti-CCL2 (1:200, ab25124, Abcam, Cambridge, UK), anti-CD45 (1:300, GB115428, Servicebio), anti-CD31 (1:2000, ab182981, Abcam), and anti-s100a4 (1:2000, GB11397, Servicebio). Following elution, the sections underwent sequential reactions with fluorescent secondary antibodies (1:1000, GB23303, Servicebio) for 50 min, shielded from the light. After a final rinsing step, DAPI dye was briefly applied briefly to the tissue sections, which were then dehydrated, sealed, and examined under light microscopy. For cellular immunofluorescence, cells were initially cultured in 48-well plates until the intervention concluded. Samples were washed twice with PBS, fixed in 4% paraformaldehyde for 10 min, permeabilized with 0.1% PBST (PBS containing 0.1% Triton X-100 [9002-93-1, Beijing Solarbio Science & Technology Co., Ltd., Beijing, China]), and blocked with 1% bovine serum albumin (BSA, GC305006, Servicebio). Subsequently, cells were treated with anti-CCR2 and anti-CCL2 antibodies, incubated overnight at 4 °C, washed, and exposed to fluorescent secondary antibodies in the dark for 30 min. After additional washing, 4′,6-diamidino-2-phenylindole (DAPI) stain was applied for 10 min, followed by a final rinse and examination under an optical microscope.

2.8 Cell Culture

Human monocytic leukemia cells were sourced from Wuhan Punosai Life Science and Technology Co., Ltd. All cell lines underwent validation by STR profiling and tested negative for mycoplasma contamination. Cells were cultured in a humidified incubator at 37 °C with 5% CO_2. Initially, THP-1 cells were induced into M0 adherent morphology by treating them with 100 ng/mL phorbol 12-myristate 13-acetate (PMA, P8139, Sigma-Aldrich, Darmstadt, Germany) for 48 hours. The cells were then divided into four groups for different interventions: NC group, LPS group (100 ng/mL), CCL2 group (100 ng/mL), and LPS+CCL2 group, with LPS (100 ng/mL) serving as the positive control. Finally, cell lysates analyzed using RT-qPCR and Western blotting to assess the expression of CCR2 and CCL2, supplemented by immunofluorescence.

2.9 Cell Transfection

The THP-1 cells were seeded at a density of 1×10^6 cells per well in a six-well plate and treated with PMA (Sigma) for 48 h to induce differentiation into M0 macrophages. To suppress *CCR2* expression, three siRNAs provided by a commercial company (Hanbio Biotechnology Co.Ltd, Shanghai, China) were used following their transfection instructions. Transfection efficiency was confirmed initially (**Supplementary Fig. 1**), and subsequently, one of the siRNAs was selected for further experiments (5′-CAGGAAUCAUCUUUACUAATT-3′; 5′-UUAGUAAAGAUGAUUCCUGTT-3′). The se-

quence of si-NC is (5′-UCUCCGAACGUCACGUTT-3′; 5′-ACUGACACGUUCGGAGAATT-3′). Following treatment with 100 ng/mL PMA for 48 h, siRNA was used to silence *CCR2* expression, and the cells were then randomly divided into four groups: NC group, si-NC group, si-NC+CCL2 group, and si-CCR2+CCL2 group for transfection. After completing the transfection, cells were further treated with CCL2 (100 ng/mL). Finally, subsequent experiments were conducted.

Table 1. Sequences of primers used in RT-qPCR.

Gene (rat)		(5′-3′)
Tnf-α	Forward	GCGTGTTCATCCGTTCTCTAC
	Reverse	GTCTCGTGTGTTTCTGAGCAT
Il-6	Forward	CCGGAGAGGAGACTTCACAGAGGA
	Reverse	AGCCTCCGACTTGTGAAGTGGTATA
Tgf-β	Forward	GACCGCAACAACGCAATCTATGAC
	Reverse	CTGGCACTGCTTCCCGAATGTC
Ccl2	Forward	CTCACCTGCTGCTACTCATTCACTG
	Reverse	CTTCTTTGGGACACCTGCTGCTG
Ccr2	Forward	GCCACCACACCGTATGACTATGATG
	Reverse	AGCAGGAAGAGCAGGTCAGAGATG
Cd68	Forward	CTCTTGCTGCCTCTCATCATTGG
	Reverse	GCTGGTAGGTTGATTGTCGTCTC
Col1a1	Forward	TGTTGGTCCTGCTGGCAAGAATG
	Reverse	GTCACCTTGTTCGCCTGTCTCAC
Col3a1	Forward	AGTCGGAGGAATGGGTGGCTATC
	Reverse	CAGGAGATCCAGGATGTCCAGAGG
β-actin	Forward	GGAGATTACTGCCCTGGCTCCTA
	Reverse	GACTCATCGTACTCCTGCTTGCTG
Gene (humam)		(5′-3′)
CCL2	Forward	ACCAGCAGCAAGTGTCCCAAAG
	Reverse	TTTGCTTGTCCAGGTGGTCCATG
CCR2	Forward	CCAACGAGAGCGGTGAAGAAGTC
	Reverse	CGAGTAGAGCGGAGGCAGGAG
CD86	Forward	TGCTCATCTATACACGGTTACC
	Reverse	TGCATAACACCATCATACTCGA
TNF-α	Forward	CCTCATCTACTCCCAGGTCCTCTTC
	Reverse	TCTGGTAGGAGACGGCGATGC
IL-6	Forward	GCCTTCGGTCCAGTTGCCTTC
	Reverse	GTTCTGAAGAGGTGAGTGGCTGTC
GAPDH	Forward	TGACATCAAGAAGGTGGTGAAGCAG
	Reverse	GTGTCGCTGTTGAAGTCAGAGGAG

RT-qPCR, real time-quantitative polymerase chain reaction; TNF-α, tumor necrosis factor-α; IL-6, Interleukin 6; TGF-β, Transforming growth factor-β; CCL2, C-C motif chemokine ligand 2; COL1A1, collagen type I alpha 1; COL3A1, collagen type III alpha 1; CCR2, C-C chemokine receptor type 2; GAPDH, Glyceraldehyde-3-phosphate dehydrogenase.

2.10 Enzyme-Linked Immunosorbent Assay (ELISA)

The concentration of CCL2 in rat serum and levels of Interleukin-12A (IL-12A), IL-6, and IL-1β in cell supernatants were measured using enzyme-linked immunosorbent assay (ELISA) kits (GEH0009, GEH0001, GEH0002, Servicebio, Wuhan, China). Each sample was tested in triplicate, and the absorbance of each well at 450 nm was measured using an enzyme reader (Thermo Fisher Scientific, Inc., Waltham, MA, USA) following the manufacturer's protocol.

2.11 Statistical Analysis

The number of animals used in the *in vivo* experiments was denoted as "n". For the *in vitro* investigations, "n" represented the number of experiments conducted. Statistical analyses were performed using GraphPad Prism 9.5 (GraphPad Software, San Diego, CA, USA) and SPSS 27 (IBM-SPSS Statistics, Chicago, IL, USA). Data were expressed as mean ± SEM, and differences among three or more groups were analyzed using ANOVA. Statistical significance was set at $p < 0.05$.

3. Results

3.1 CCR2 and CCL2 Positive Cells Expressed on Valves of RHD Patients

The co-expression of CD68, CCR2, and COL1A revealed by immunofluorescence is shown in (**Supplementary Fig. 2A**). CCL2 was also expressed in leukocytes marked with CD45, endothelial cells marked with CD31, and fibroblasts marked with s100a4 (**Supplementary Fig. 2B**). These findings provide evidence for the presence of $CCR2^+$ macrophages in the valves of RHD patients, notably in close proximity to fibrin. The expression of CCL2 on endothelial cells and fibroblasts suggests a potential mechanism for recruiting $CCR2^+$ macrophages from the bloodstream to the valve site.

3.2 CCR2 Antagonist Treatment of RHD Rats Ameliorates Valve Inflammation and Fibrosis

Key observations included a notable increase in the infiltration of inflammatory cells within RHD rat valves, as evidenced by HE stains (Fig. 1A), and exacerbation of valve fibrosis in the RHD group, observed in Sirius red polarized light images (Fig. 1B). Remarkably, these adverse changes were significantly mitigated following administration of Rs-504393. Analysis via RT-qPCR (Fig. 2A) and western blot (Fig. 2C) in RHD rats revealed heightened activation of the CCL2/CCR2 axis, elevated levels of pro-inflammatory and pro-fibrotic cytokines (*TNF-α*, *IL-6*, *TGF-β*, *CCL2*, *CCR2*, *CD68*, *COL1A1*, and *COL3A1*), and increased expression offibrotic markers such as COL1A, COL3A, and α-SMA. Treatment with Rs-504393 effectively attenuated these alterations. These findings underscore the activation of the CCL2/CCR2 axis in RHD pathology. Moreover, CCR2 antagonists demonstrated therapeutic efficacy by effectively blocking the CCL2/CCR2 axis, thereby ameliorating inflammatory infiltration and valvular fibrosis in RHD

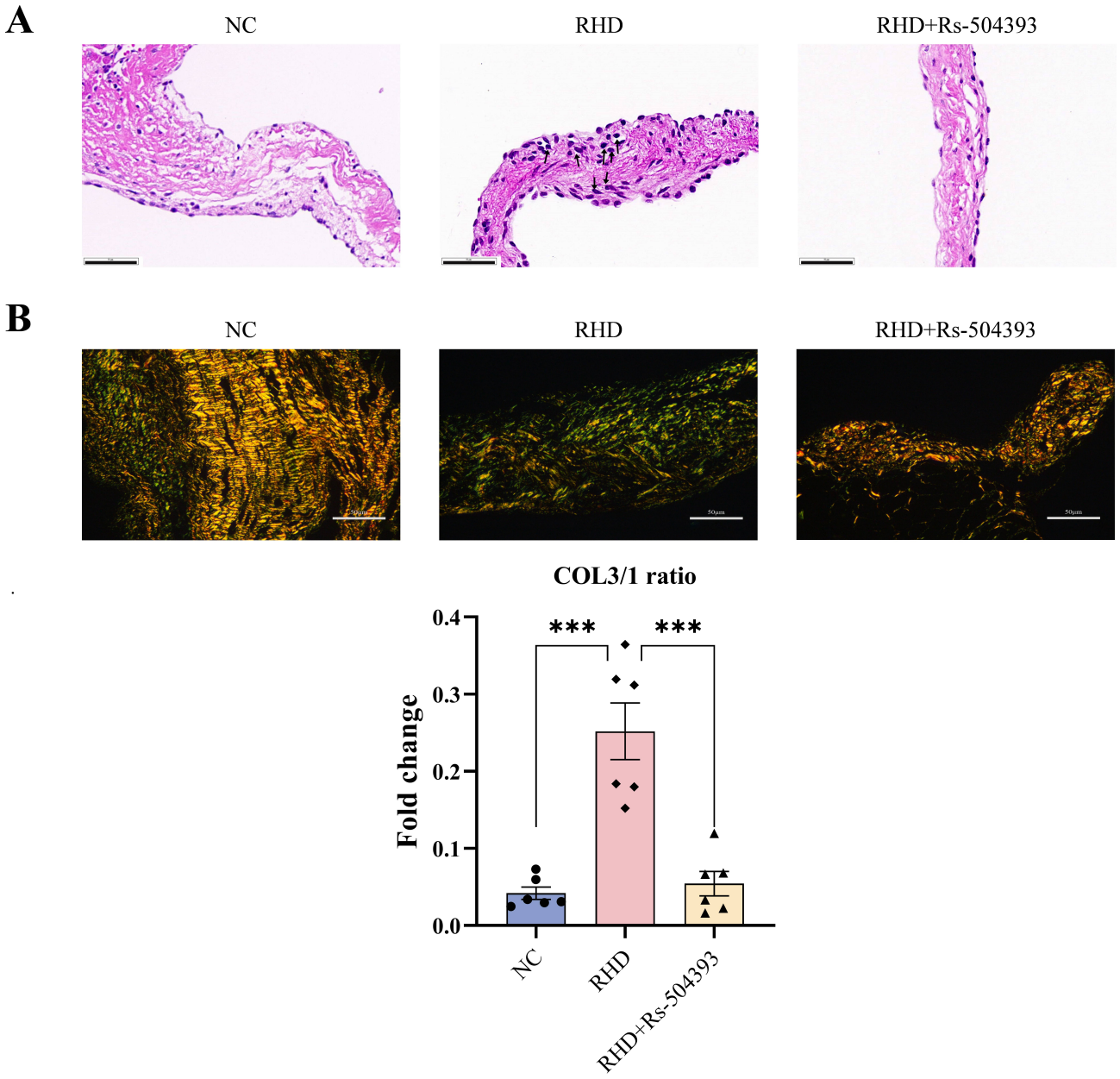

Fig. 1. Pathological staining in each rat group. (A) Inflammatory changes in the valves of the NC group, RHD group, and RHD+Rs-504393 treatment group were observed through HE staining, with images captured at the original magnification of ×400, scale bar = 50 µm, n = 6. (B) Upper Image: Sirius Red staining captured under polarized light displays the expression of type I collagen fibers (COL1A, red or yellow light) and type III collagen fibers in the NC group, RHD group, and RHD+Rs-504393 treatment group, with images captured at the original magnification of ×400, scale bar = 50 µm, n = 6. Lower Image: Statistical data of the COL3A/COL1A ratio for each group, where a higher ratio indicates a greater degree of fibrosis. Data are presented as mean ± standard deviation. ***$p < 0.001$. NC, negative control; RHD, rheumatic heart disease; HE, hematoxylin-eosin staining.

rats. Importantly, there were no statistically significant differences in weight changes observed among the experimental groups.

3.3 The CCR2 Antagonist Rs-504393 Acts by Reducing CCR2 Macrophage Infiltration

Protein blot analysis (Fig. 2C), ELISA (Fig. 2B), RT-qPCR (Fig. 2A) and immunohistochemistry (Fig. 3) conducted on the valves of RHD rats showed a significant upregulation in CCL2 expression and a notable increase in macrophage numbers compared to controls. Treatment with Rs-504393 resulted in a marked reduction in the total count of CD68-labeled macrophages, specifically decreasing both $CCR2^+$ and M1-type macrophages. Statistical analysis of the immunohistochemistry showed a minimal change in the number of M2-labeled macrophages,

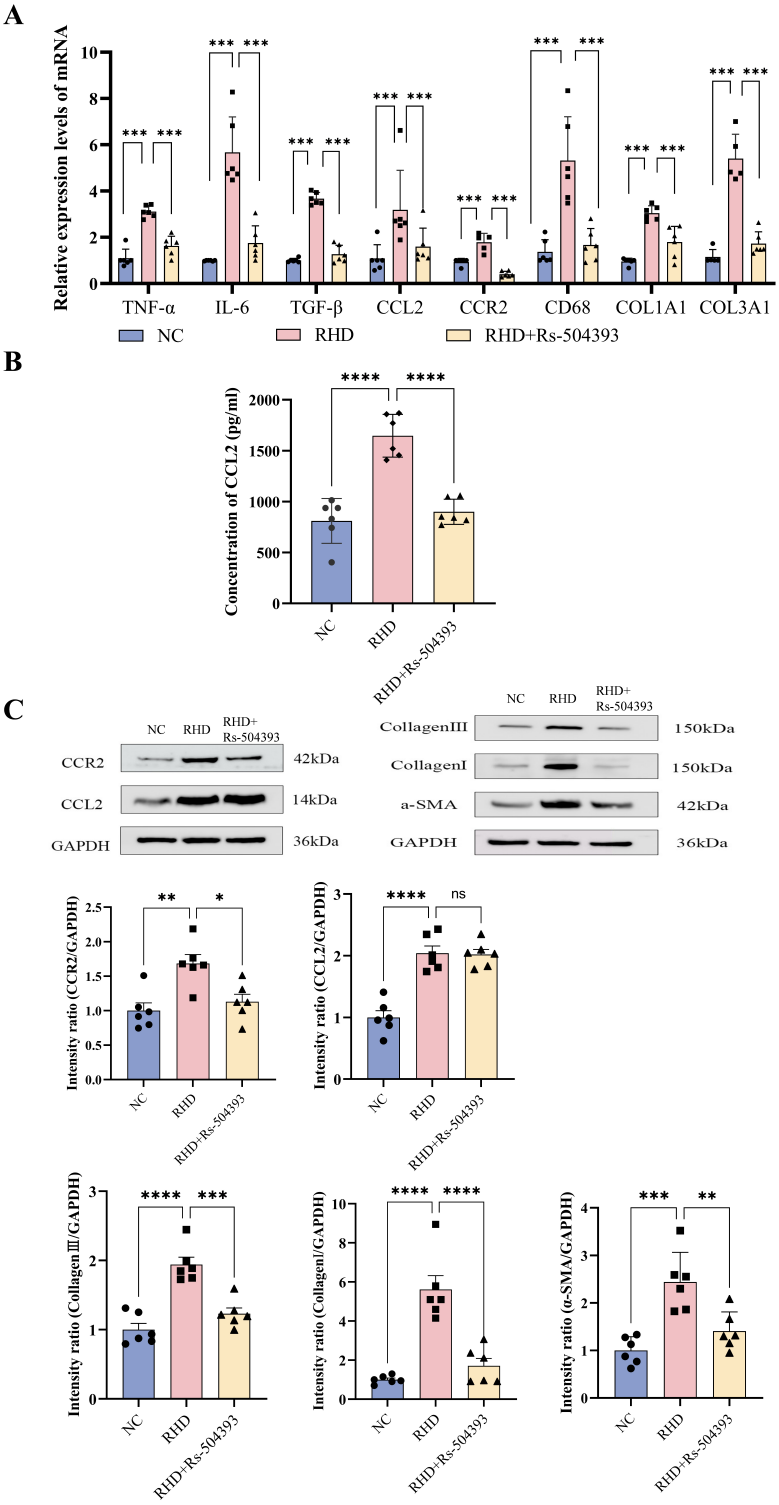

Fig. 2. Changes in the expression levels of pro-inflammatory cytokines, fibrosis markers, and macrophage markers in valve tissues after Rs-504393 treatment. (A) RT-qPCR was employed to detect mRNA levels of *TNF-α*, *IL-6*, *TGF-β*, *CCL2*, *CCR2*, *CD68*, *COL1A1*, and *COL3A1* in valve tissues. (B) CCL2 levels in rat serum were assessed using ELISA. (C) Upper panel: Western blotting analysis of the expression levels of CCL2, CCR2, COL1A1, COL3A1, and α-SMA in valve tissues. Lower panel: Relative expression levels in each group were analyzed using ImageJ. Data are presented as mean ± SD, n = 6. ns: Not Statistically Significant, *$p < 0.05$, **$p < 0.01$, ***$p < 0.001$, ****$p < 0.0001$. RT-qPCR, Quantitative reverse transcription polymerase chain reaction; *TNF-α*, tumor necrosis factor-α; *IL-6*, Interleukin 6; *TGF-β*, Transforming growth factor-β; CCL2, C-C motif chemokine ligand 2; CCR2, C-C chemokine receptor type 2; COL1A1, collagen type I alpha 1; COL3A1, collagen type III alpha 1; α-SMA, α-smooth muscle actin; ELISA, enzyme-linked immunosorbent assay.

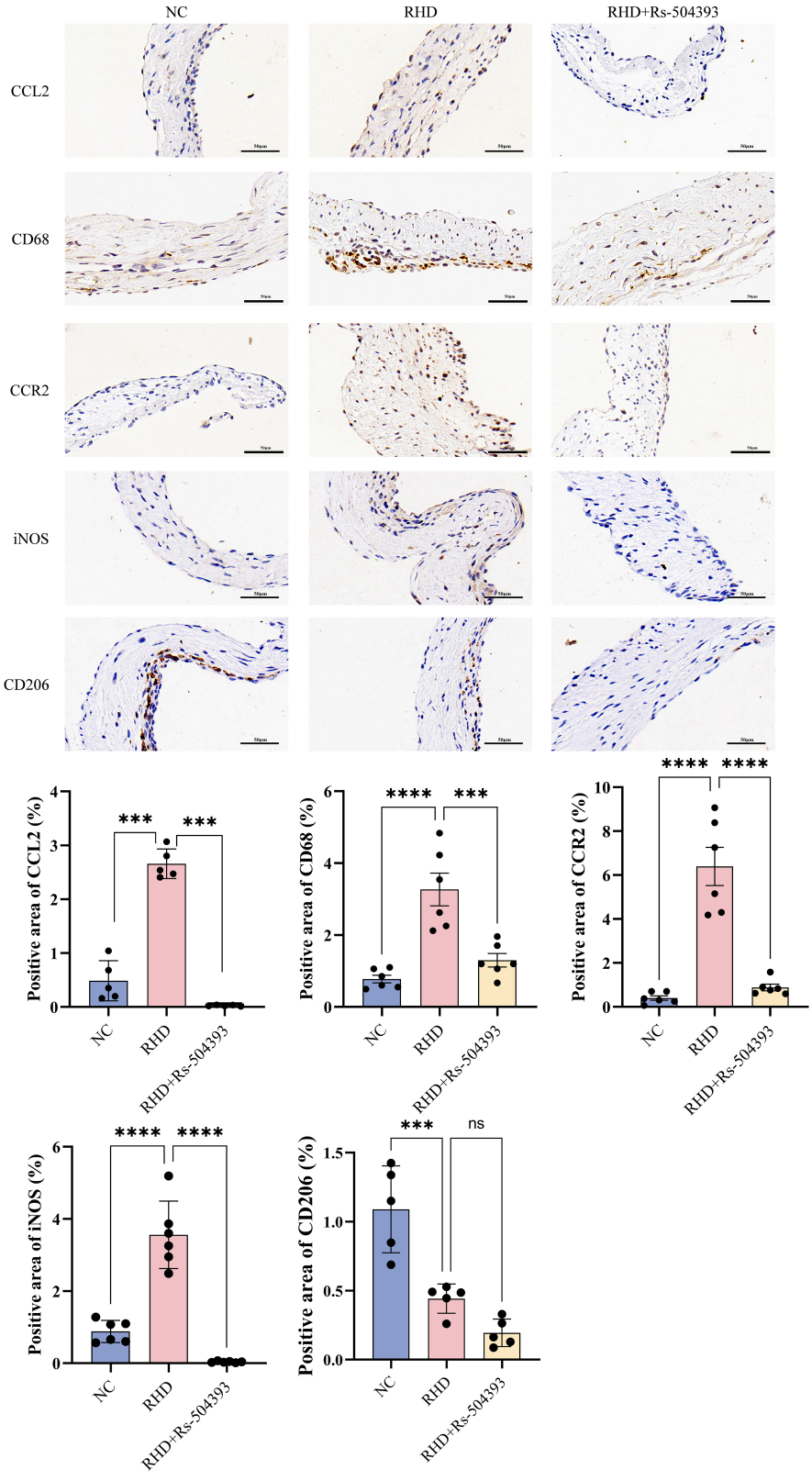

Fig. 3. Immunohistochemistry reveals infiltration of different macrophage subtypes in each group. Upper Panel: Immunohistochemical expression of CCL2, CD68, CCR2, iNOS, and CD206 in the NC group, RHD group, and RHD+Rs-504393 treatment group. Images were captured at the original magnification of ×400, scale bar = 50 µm. Lower Panel: Relative positive areas analyzed through Image-pro plus 6.0 (Media Cybernetics, Rockville, MD, USA). Data are presented as mean ± standard deviation, n = 6. ns: Not Statistically Significant, ***$p < 0.001$, ****$p < 0.0001$. iNOS, inducible nitric oxide sythase.

potentially attributable to the acute nature of this experimental model. These findings collectively suggest that Rs-504393 treatment attenuates inflammation and fibrosis in rheumatic rat valves by reducing the infiltration of $CCR2^+$ macrophages.

3.4 CCL2 Recombinant Protein Intervention in THP-1 Cells Promotes their M1 Polarization

Various concentrations of CCL2 were applied to intervene on M0 macrophages for 24h, and the optimal concentration that maximized CCR2 expression was determined to be 100 ng/mL based on the CCK8 assay (Fig. 4A) and RT-qPCR experiment (Fig. 4B). RT-qPCR (Fig. 4C) and flow cytometry (Fig. 4D) demonstrated elevated levels of inflammatory factors (*CCL2*, *IL-6*, *TNF-*α, *CCR2*, and *CD86*), along with increased expression of CCR2 and the M1 macrophage marker CD86 in both the LPS and CCL2 groups compared to levels observed in the NC group. Furthermore, CCL2 amplified the pro-inflammatory and M1 polarization effects induced by LPS. Immunofluorescence analysis (Fig. 4E,F and **Supplementary Fig. 3A,B**) corroborated these findings, showing consistent increases in CCR2 and CCL2 expression. Specifically, fluorescence intensity of both CCR2 and CCL2 was higher in the LPS and CCL2 groups compared to the NC group. Moreover, fluorescence intensity was further elevated in the LPS+CCL2 group compared to both the LPS alone and CCL2 alone groups.

3.5 siRNA Knockdown of CCR2 in THP-1 Cells Inhibits the Pro-M1 Polarizing Effect of CCL2 Recombinant Protein

RT-qPCR analysis (Fig. 5A) showed that the mRNA expression levels of signature indicators of M1-type macrophages (including *IL-6*, *TNF-*α, and *CD86*) and *CCL2*/*CCR2* were increased in the si-NC+CCL2 group compared to the si-NC group. Conversely, the mRNA expression levels of *IL-6*, *TNF-*α, *CD86*, and *CCL2*/*CCR2* were significantly reduced in the si-CCR2+CCL2 group compared to the si-NC+CCL2 group. Immunofluorescence analysis (Fig. 5B,C and **Supplementary Fig. 3C,D**) further confirmed that the fluorescence intensity of CCL2 and CCR2 was lower in the si-CCR2+CCL2 group compared to the si-NC+CCL2 group.

The ELISA results from cell supernatants showed elevated levels of inflammatory factors such as IL-12A, IL-6, and IL-1β in the supernatants of the si-NC+CCL2 group compared to the si-NC group. Conversely, after silencing *CCR2*, the levels of these inflammatory factors decreased in the supernatants of the si-CCR2+CCL2 group (Fig. 6A). This indicates that silencing *CCR2* expression in macrophages significantly inhibits the pro-inflammatory effect of CCL2 protein on macrophages. Additionally, protein blotting experiments revealed increased expression levels of CCL2, CCR2, and CD86 in macrophages of the si-NC+CCL2 group compared to the si-NC group. Following *CCR2* silencing, the expression of these proteins was significantly reduced in the si-CCR2+CCL2 group compared to the si-NC+CCL2 group (Fig. 6B). These results demonstrate that silencing *CCR2* expression in macrophages not only prevents macrophage polarization towards M1 but also reduces the expression of CCL2/CCR2 proteins.

4. Discussion

This study investigated macrophage recruitment and polarization both *in vivo* and *in vitro* to assess the impact of inhibiting the CCL2/CCR2 axis on the progression of RHD. We observed an expanded macrophage population in the valves of Lewis rats infected with GAS for 8 weeks, characterized by a significant increase in the proportion of the M1 phenotype and only a minimal change in the M2 phenotype. Elevated levels of the monocyte chemotactic factors and their chemokine receptors were identified as primary contributors to the increased macrophage presence in the valves. Additionally, we demonstrated a correlation between macrophage infiltration in the valves of RHD rats and the development of fibrosis. Blocking the CCL2/CCR2 axis with the CCR2-specific antagonist Rs-504393 resulted in a substantial reduction in macrophage numbers in RHD rats valves, along with a significant decrease in valve inflammation and fibrosis. *In vitro* experiments simulating CCL2 action on macrophages revealed that the CCL2 protein promotes polarization towards the pro-inflammatory M1 type. However, this effect was attenuated when *CCR2* was silenced in macrophages using small interfering RNA. Together, these findings suggest that macrophage recruitment and polarization play a crucial role in RHD progression, highlighting them as potential targets for treating valve fibrosis associated with RHD.

Effective tissue repair following injury is crucial for the survival of all organisms [23]. After tissue damage, various immune cells are recruited to the site to clear cellular debris and infectious microorganisms, thereby coordinating the tissue repair response. The extent and duration of this repair response may vary, influencing the final outcome. While enhancing the inflammatory response is beneficial, it can also activate fibrotic reactions leading to excessive accumulation of collagenous connective tissue and subsequent organ dysfunction [24]. There is evidence that macrophages play a critical regulatory role at all stages of repair and fibrosis [25]. In cardiac tissue, a significant population of resident macrophages exists, with increases during injury due to infiltration of circulating monocytes [26]. Circulating monocytes also serve as a source of myofibroblasts in the injured heart, contributing to cardiac repair [27]. Recent studies in mouse hearts following transverse aortic constriction surgery have shown that macrophages derived from recruited monocytes stimulate fibrosis. In contrast, resident macrophages inhibit cardiac fibrosis, their expression of CCR2 helps categorize them as either resident

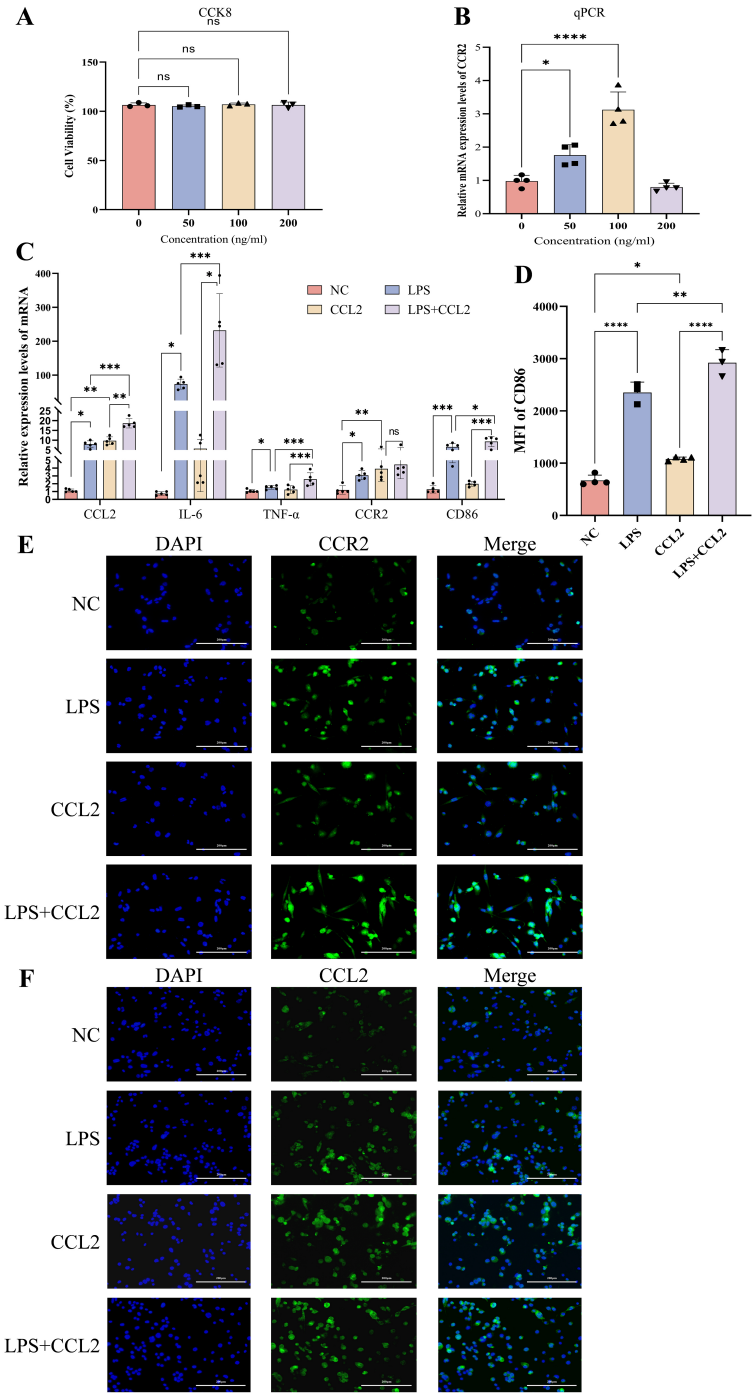

Fig. 4. Expression of cytokines and M1 phenotype after intervention with recombinant CCL2 (100 ng/mL) and LPS (100 ng/mL) in THP-1 cells. (A) CCK8 assay assessing the impact on cell viability when THP-1 cells in the M0 state were intervened with different concentrations of recombinant CCL2 for 24 hours, n = 4. (B) RT-qPCR measuring the expression levels of *CCR2* in M0 state THP-1 cells intervened with different concentrations of recombinant CCL2, n = 4. (C) RT-qPCR detecting the mRNA levels of *CCL2*, *IL-6*, *TNF-α*, *CCR2*, and *CD86* in THP-1 cells intervened with recombinant CCL2 (100 ng/mL), LPS (100 ng/mL), and CCL2+LPS, n = 4. (D) Flow cytometry measuring the average fluorescence intensity of CD86 in each intervention group, n = 4. (E) Immunofluorescence showing the fluorescence intensity of CCR2 (green light) in each intervention group, images were captured at the original magnification of ×200, scale bar = 200 μm, n = 3. (F) Immunofluorescence showing the fluorescence intensity of CCL2 (green light) in each intervention group, images were captured at the original magnification of ×200, scale bar = 200 μm, n = 3. Data are presented as mean ± SD. ns: Not Statistically Significant, *$p < 0.05$, **$p < 0.01$, ***$p < 0.001$, ****$p < 0.0001$. LPS, lipopolysaccharide; MFI, mean fluorescence intensity; CCK8, cell counting kit-8.

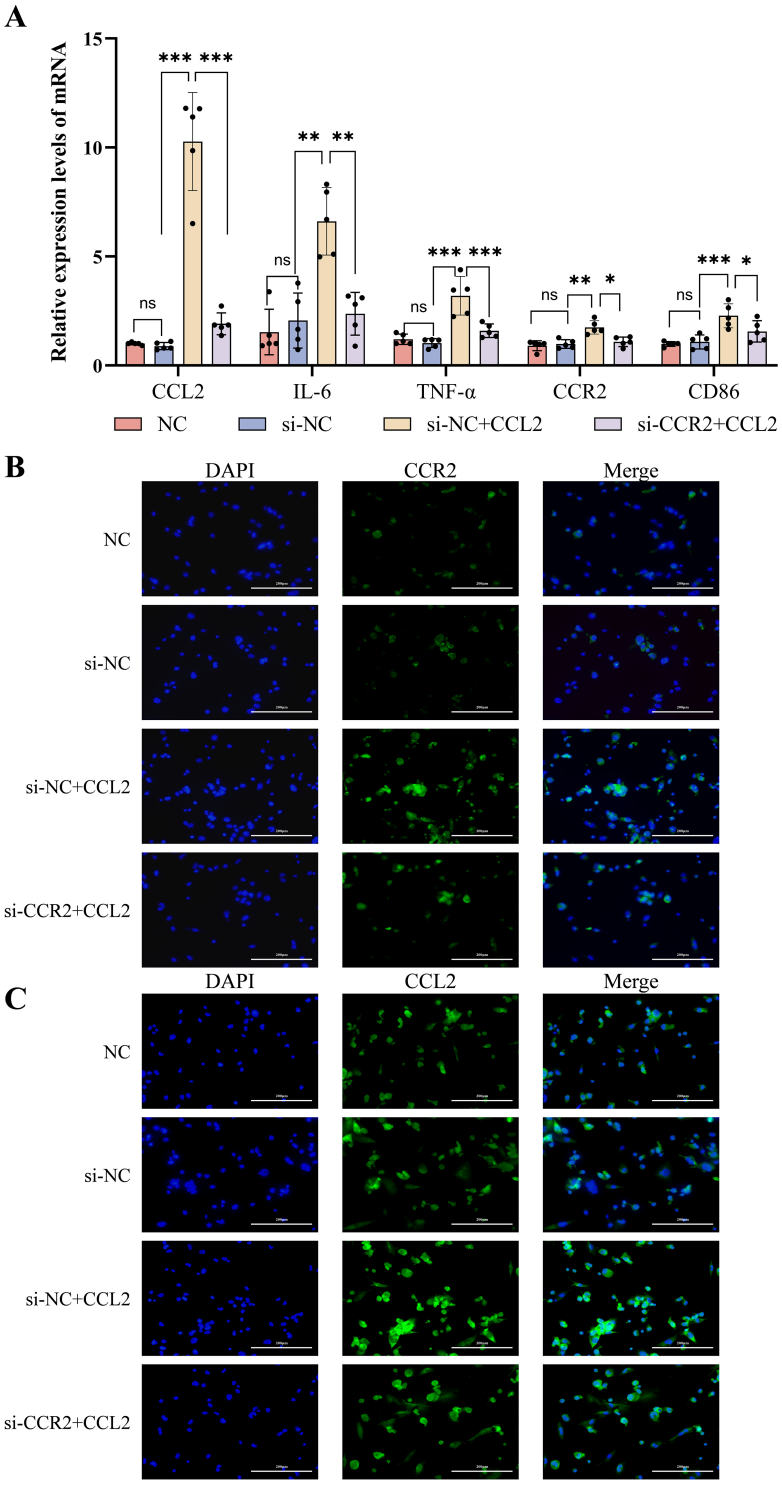

Fig. 5. Expression of inflammatory cytokines and M1 phenotype molecules after knockdown of *CCR2* in THP-1 cells using siRNA, followed by intervention with CCL2. (A) RT-qPCR detecting the mRNA levels of *CCL2*, *IL-6*, *TNF-α*, *CCR2*, and *CD86* in THP-1 cells with siRNA-*CCR2* knockdown intervened with recombinant CCL2 (100 ng/mL), n = 4. (B) Immunofluorescence showing the fluorescence intensity of CCR2 (green light) in each intervention group, images were captured at the original magnification of ×200, scale bar = 200 μm, n = 3. (C) Immunofluorescence showing the fluorescence intensity of CCL2 (green light) in each intervention group, images were captured at the original magnification of ×400, scale bar = 200 μm, n = 3. Data are presented as mean ± SD. ns: Not Statistically Significant, *$p < 0.05$, **$p < 0.01$, ***$p < 0.001$. si-NC, small interfering-negative control; si-CCR2, small interfering-C-C chemokine receptor type 2.

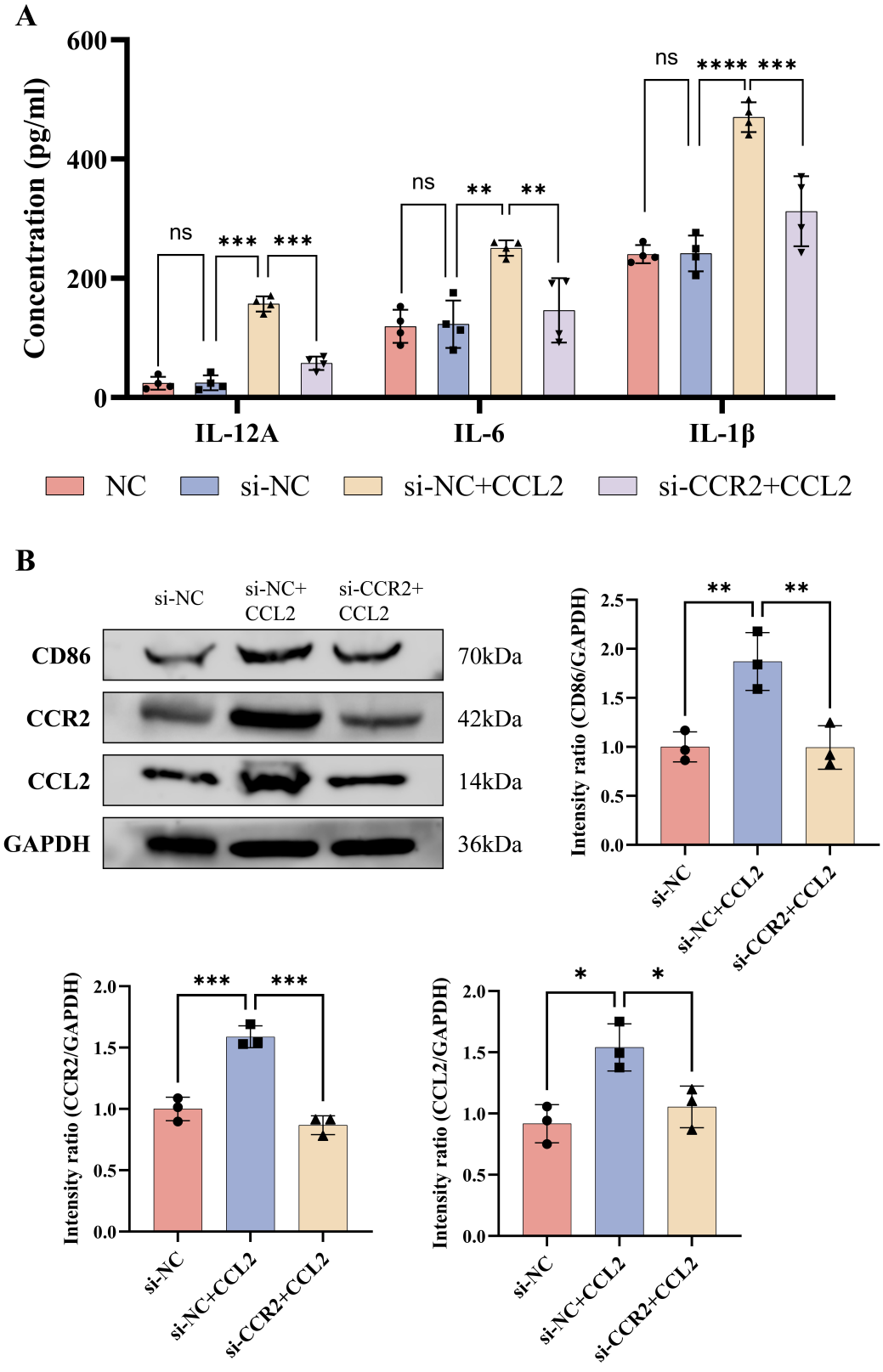

Fig. 6. Silencing *CCR2* in THP-1 cells followed by treatment with CCL2 was conducted to assess the levels of inflammatory cytokines in the cell supernatants and the expression of CCL2, CCR2, and CD86 in THP-1 cells. (A) ELISA was used to measure the levels of IL-12A, IL-6, and IL-1β in the cell supernatants of each group, n = 4. (B) Western blotting was performed to analyze the protein expression levels of CCL2, CCR2, and CD86 in each group, n = 3. Data are presented as mean ± SD. ns: Not Statistically Significant, *$p < 0.05$, **$p < 0.01$, ***$p < 0.001$, ****$p < 0.0001$.

(CCR2-) or circulating-derived ($CCR2^+$) types [28]. Furthermore, in Marfan's syndrome (MFS), CCR2 deficiency in monocytes inhibits macrophage recruitment. Studies in mice have demonstrated that this protects against the progression of mucoid valve degeneration, resulting in minimal leaflet thickening and preserved stromal integrity [29]. Numerous studies have reported that $CCR2^+$ mesenchymal macrophages play a role in promoting pulmonary fibrosis, with an increase in CCR2-dependent monocytes and mesenchymal macrophages found in the lungs of patients with this condition [30,31]. These mesenchymal macrophages produce factors that induce fibroblast recruitment and collagen production, highlighting their involvement in the profibrotic process [32]. Importantly, studies using CCR2-deficient mouse models have shown significantly reduced pulmonary fibrosis [33,34]. These findings are consistent with our observations in RHD rats, where an increase in CCR2 macrophages correlates with inflammation and fibrosis of the valves, both of which are significantly reduced by inhibiting the aggregation of CCR2 macrophages. This suggests an indispensable role for CCR2 macrophages in tissue repair and fibrosis.

The migration of CCR2-expressing cells from the circulation into specific tissues and organs during disease progression has been extensively studied across various conditions. CCR2 binds to several chemokines, including CCL2, CCL7, CCL8, CCL11, CCL13, CCL16, and CCL26 [35,36], with CCL2 recognized as its primary ligand [37]. The amino-terminal region of CCL2 plays a crucial role in determining binding affinity and signaling selectivity for CCR2 [38]. In our study of rats with RHD, we observed a significant elevation of CCL2 levels in both tissue and serum, potentially contributing to increased cell numbers in the valves. Research on osteoarthritis has highlighted that the CCL2/CCR2 axis, rather than CCL5/CCR5, mediates monocyte recruitment, inflammation, and cartilage destruction [13]. In atherosclerosis, CCL2 facilitates the movement of inflammatory monocytes between the bone marrow, circulation, and atherosclerotic plaques by binding to CCR2 [35,39]. Studies across different tumors have similarly emphasized the critical role of the CCL2/CCR2 axis in orchestrating the migration of immune cells into the tumor microenvironments [40]. CCL2 expression is widespread across various cell types, including stromal cells, smooth muscle cells, fibroblasts, leukocytes, endothelial cells, and tumor cells [41–43]. Our experiments identified CCL2 expression in leukocytes, endothelial cells, and fibroblasts within the valves of RHD patients. These findings underscore the potential of targeting the CCL2/CCR2 axis as a therapeutic strategy in numerous diseases.

The prevalence of RHD remains high in some populations in both developing and developed countries, with global estimates indicating that 40.5 million people currently suffer from RHD and 306,000 people die from the disease each year [3]. Despite this high prevalence and mortality rate, the pathogenesis of the disease remains poorly understood. Previous studies have focused on the pathogenicity of GSA, the role of various cytokines, the function of T lymphocytes during valve injury, and the involvement of macrophages in RHD, including their infiltration pathways into the valve [7,44,45]. Our findings may therefore shed light on these aspects and lay the groundwork for further investigations into the pathogenesis of RHD, potentially confirming the CCL2/CCR2 axis as a therapeutic target to mitigate macrophage recruitment in heart valves.

We are also concerned about the the investigation of targeted therapeutic agents against the CCL2/CCR2 signaling axis in various autoimmune diseases. A randomized controlled trial showed that treatment of rheumatoid arthritis with a human anti-CCL2 monoclonal antibody (ABN912) did not result in clinical or immunohistological improvement, possibly due to a significant increase in serum total CCL2/Monocyte Chemotactic Protein 1 (MCP-1) levels observed after ABN912 treatment [46]. In another study, patients with rheumatoid arthritis treated with an anti-CCR2 antibody (MLN1202) in a phase IIa clinical trial did not show significant clinical improvement compared to placebo [47]. Rs-504393, a selective CCR2 antagonist inhibiting ERK1/2 activation, has shown promise in early-stage osteoarthritis by reducing pain [48]. Additionally, the humanized anti-CCR2 monoclonal antibody MLN1202 has been effective in reducing brain lesions in patients with multiple sclerosis [49]. The potential therapeutic role of these drugs targeting the CCL2/CCR2 axis in treating RHD requires validation through further animal and clinical trials. We regret that we were unable to collect valvular tissue samples from RHD patients and controls for validation, and that we could not utilize a CCL2/CCR2 knockout animal model for further validation. Future studies could enhance this research by incorporating larger population samples and employing knockout animal models.

5. Conclusions

In conclusion, this study demonstrated that pharmacological blockade of the CCR2 signaling pathway with Rs-504393 significantly reduced the severity of valve inflammation and fibrosis in rats with RHD. This effect was attributed to mechanisms involving reduced macrophage accumulation in the valves.

Availability of Data and Materials

The raw data supporting the conclusions of this article will be made available by the correspondence author (zengzhiyu@gxmu.edu.cn) on reasonable request.

Author Contributions

ZYZ, FH and YX conceived and designed the study. LB and YL participated in the experimental design. LB, YL, CHL and ZRL conducted the experiments. LB, YL

and ZYM analyzed the data. LB and YL drafted the manuscript. All authors contributed to editorial changes in the manuscript. All authors approved the final version. All authors agree to be accountable for all aspects of the work to ensure that questions related to the accuracy or integrity of any part of the work are appropriately investigated and resolved.

Ethics Approval and Consent to Participate

The protocol involving animals and patients has been approved by the Medical Ethics Committee of the First Affiliated Hospital of Guangxi Medical University (Approval Number: 2023-E751-01), and all study participants provided written informed consent.

Acknowledgment

We thank the Department of Cardiothoracic Surgery of the First Affiliated Hospital of Guangxi Medical University for providing the valve specimens. The authors would like to express their gratitude to EditSprings (https://www.editsprings.cn) for the expert linguistic services provided.

Funding

This study was supported by the National Natural Science Foundation of China (Grant No. 81960082), Guangxi Key Laboratory Base of Precision Medicine Control and Prevention of Cardiovascular and Cerebrovascular Diseases (Grant No. 17-259-85), and Guangxi Clinical Research Center of Cardiovascular and Cerebrovascular Diseases (Grant No. AD17129014).

Conflict of Interest

The authors declare no conflict of interest.

Supplementary Material

Supplementary material associated with this article can be found, in the online version, at https://doi.org/10.31083/j.fbl2908303.

References

[1] Dougherty S, Okello E, Mwangi J, Kumar RK. Rheumatic Heart Disease: JACC Focus Seminar 2/4. Journal of the American College of Cardiology. 2023; 81: 81–94.

[2] Carapetis JR, McDonald M, Wilson NJ. Acute rheumatic fever. Lancet. 2005; 366: 155–168.

[3] Watkins DA, Roth GA. Global Burden of Rheumatic Heart Disease. The New England Journal of Medicine. 2018; 378: e2.

[4] Moudgil KD, Choubey D. Cytokines in autoimmunity: role in induction, regulation, and treatment. Journal of Interferon & Cytokine Research. 2011; 31: 695–703.

[5] Rojas M, Restrepo-Jiménez P, Monsalve DM, Pacheco Y, Acosta-Ampudia Y, Ramírez-Santana C, *et al*. Molecular mimicry and autoimmunity. Journal of Autoimmunity. 2018; 95: 100–123.

[6] Ellis NMJ, Li Y, Hildebrand W, Fischetti VA, Cunningham MW. T cell mimicry and epitope specificity of cross-reactive T cell clones from rheumatic heart disease. Journal of Immunology. 2005; 175: 5448–5456.

[7] Faé KC, da Silva DD, Oshiro SE, Tanaka AC, Pomerantzeff PMA, Douay C, *et al*. Mimicry in recognition of cardiac myosin peptides by heart-intralesional T cell clones from rheumatic heart disease. Journal of Immunology. 2006; 176: 5662–5670.

[8] Gorton D, Blyth S, Gorton JG, Govan B, Ketheesan N. An alternative technique for the induction of autoimmune valvulitis in a rat model of rheumatic heart disease. Journal of Immunological Methods. 2010; 355: 80–85.

[9] Deng F, Chen W, Liu L, Wang LM, Chen X. The expression and molecular mechanism of M1 macrophages in rheumatic valvular disease. Zhonghua Wai Ke Za Zhi. 2012; 50: 933–937. (In Chinese)

[10] Hobday PM, Auger JL, Schuneman GR, Haasken S, Verbeek JS, Binstadt BA. Fcγ receptor III and Fcγ receptor IV on macrophages drive autoimmune valvular carditis in mice. Arthritis & Rheumatology (Hoboken, N.J.). 2014; 66: 852–862.

[11] Zhu S, Liu M, Bennett S, Wang Z, Pfleger KDG, Xu J. The molecular structure and role of CCL2 (MCP-1) and C-C chemokine receptor CCR2 in skeletal biology and diseases. Journal of Cellular Physiology. 2021; 236: 7211–7222.

[12] Flegar D, Filipović M, Šućur A, Markotić A, Lukač N, Šisl D, *et al*. Preventive CCL2/CCR2 Axis Blockade Suppresses Osteoclast Activity in a Mouse Model of Rheumatoid Arthritis by Reducing Homing of CCR2^{hi} Osteoclast Progenitors to the Affected Bone. Frontiers in Immunology. 2021; 12: 767231.

[13] Raghu H, Lepus CM, Wang Q, Wong HH, Lingampalli N, Oliviero F, *et al*. CCL2/CCR2, but not CCL5/CCR5, mediates monocyte recruitment, inflammation and cartilage destruction in osteoarthritis. Annals of the Rheumatic Diseases. 2017; 76: 914–922.

[14] Zoshima T, Baba T, Tanabe Y, Ishida Y, Nakatani K, Nagata M, *et al*. CCR2- and CCR5-mediated macrophage infiltration contributes to glomerular endocapillary hypercellularity in antibody-induced lupus nephritis. Rheumatology. 2022; 61: 3033–3048.

[15] Ishikawa M, Yamamoto T. Antifibrogenic effects of C-C chemokine receptor type 2 antagonist in a bleomycin-induced scleroderma model. Experimental Dermatology. 2021; 30: 179–184.

[16] Hu S, Yang M, Huang S, Zhong S, Zhang Q, Ding H, *et al*. Different Roles of Resident and Non-resident Macrophages in Cardiac Fibrosis. Frontiers in Cardiovascular Medicine. 2022; 9: 818188.

[17] Lefere S, Devisscher L, Tacke F. Targeting CCR2/5 in the treatment of nonalcoholic steatohepatitis (NASH) and fibrosis: opportunities and challenges. Expert Opinion on Investigational Drugs. 2020; 29: 89–92.

[18] Krenkel O, Puengel T, Govaere O, Abdallah AT, Mossanen JC, Kohlhepp M, *et al*. Therapeutic inhibition of inflammatory monocyte recruitment reduces steatohepatitis and liver fibrosis. Hepatology. 2018; 67: 1270–1283.

[19] Wilkening A, Krappe J, Mühe AM, Lindenmeyer MT, Eltrich N, Luckow B, *et al*. C-C chemokine receptor type 2 mediates glomerular injury and interstitial fibrosis in focal segmental glomerulosclerosis. Nephrology, Dialysis, Transplantation. 2020; 35: 227–239.

[20] Wang W, Ai J, Liao B, Xiao K, Lin L, Chen H, *et al*. The roles of MCP-1/CCR2 mediated macrophage recruitment and polarization in bladder outlet obstruction (BOO) induced bladder remodeling. International Immunopharmacology. 2021; 99: 107947.

[21] Xie X, Zhou H, Huang J, Huang H, Feng Z, Mei K, *et al*. An animal model of chronic rheumatic valvulitis induced by formalin-killed streptococci. Rheumatology International. 2010; 30: 1621–1625.

[22] Sikder S, Williams NL, Sorenson AE, Alim MA, Vidgen ME,

Moreland NJ, *et al*. Group G Streptococcus Induces an Autoimmune Carditis Mediated by Interleukin 17A and Interferon γ in the Lewis Rat Model of Rheumatic Heart Disease. The Journal of Infectious Diseases. 2018; 218: 324–335.

[23] Eming SA, Martin P, Tomic-Canic M. Wound repair and regeneration: mechanisms, signaling, and translation. Science Translational Medicine. 2014; 6: 265sr6.

[24] Eming SA, Wynn TA, Martin P. Inflammation and metabolism in tissue repair and regeneration. Science. 2017; 356: 1026–1030.

[25] Wynn TA, Barron L. Macrophages: master regulators of inflammation and fibrosis. Seminars in Liver Disease. 2010; 30: 245–257.

[26] Epelman S, Lavine KJ, Beaudin AE, Sojka DK, Carrero JA, Calderon B, *et al*. Embryonic and adult-derived resident cardiac macrophages are maintained through distinct mechanisms at steady state and during inflammation. Immunity. 2014; 40: 91–104.

[27] Möllmann H, Nef HM, Kostin S, von Kalle C, Pilz I, Weber M, *et al*. Bone marrow-derived cells contribute to infarct remodelling. Cardiovascular Research. 2006; 71: 661–671.

[28] Revelo XS, Parthiban P, Chen C, Barrow F, Fredrickson G, Wang H, *et al*. Cardiac Resident Macrophages Prevent Fibrosis and Stimulate Angiogenesis. Circulation Research. 2021; 129: 1086–1101.

[29] Kim AJ, Xu N, Umeyama K, Hulin A, Ponny SR, Vagnozzi RJ, *et al*. Deficiency of Circulating Monocytes Ameliorates the Progression of Myxomatous Valve Degeneration in Marfan Syndrome. Circulation. 2020; 141: 132–146.

[30] Misharin AV, Morales-Nebreda L, Reyfman PA, Cuda CM, Walter JM, McQuattie-Pimentel AC, *et al*. Monocyte-derived alveolar macrophages drive lung fibrosis and persist in the lung over the life span. The Journal of Experimental Medicine. 2017; 214: 2387–2404.

[31] Reyfman PA, Walter JM, Joshi N, Anekalla KR, McQuattie-Pimentel AC, Chiu S, *et al*. Single-Cell Transcriptomic Analysis of Human Lung Provides Insights into the Pathobiology of Pulmonary Fibrosis. American Journal of Respiratory and Critical Care Medicine. 2019; 199: 1517–1536.

[32] Aran D, Looney AP, Liu L, Wu E, Fong V, Hsu A, *et al*. Reference-based analysis of lung single-cell sequencing reveals a transitional profibrotic macrophage. Nature Immunology. 2019; 20: 163–172.

[33] Moore BB, Paine R, 3rd, Christensen PJ, Moore TA, Sitterding S, Ngan R, *et al*. Protection from pulmonary fibrosis in the absence of CCR2 signaling. Journal of Immunology. 2001; 167: 4368–4377.

[34] Gharaee-Kermani M, McCullumsmith RE, Charo IF, Kunkel SL, Phan SH. CC-chemokine receptor 2 required for bleomycin-induced pulmonary fibrosis. Cytokine. 2003; 24: 266–276.

[35] Georgakis MK, Bernhagen J, Heitman LH, Weber C, Dichgans M. Targeting the CCL2-CCR2 axis for atheroprotection. European Heart Journal. 2022; 43: 1799–1808.

[36] Xu M, Wang Y, Xia R, Wei Y, Wei X. Role of the CCL2-CCR2 signalling axis in cancer: Mechanisms and therapeutic targeting. Cell Proliferation. 2021; 54: e13115.

[37] Zhang H, Yang K, Chen F, Liu Q, Ni J, Cao W, *et al*. Role of the CCL2-CCR2 axis in cardiovascular disease: Pathogenesis and clinical implications. Frontiers in Immunology. 2022; 13: 975367.

[38] Huma ZE, Sanchez J, Lim HD, Bridgford JL, Huang C, Parker BJ, *et al*. Key determinants of selective binding and activation by the monocyte chemoattractant proteins at the chemokine receptor CCR2. Science Signaling. 2017; 10: eaai8529.

[39] Marchini T, Mitre LS, Wolf D. Inflammatory Cell Recruitment in Cardiovascular Disease. Frontiers in Cell and Developmental Biology. 2021; 9: 635527.

[40] Hao Q, Vadgama JV, Wang P. CCL2/CCR2 signaling in cancer pathogenesis. Cell Communication and Signaling. 2020; 18: 82.

[41] Soria G, Ben-Baruch A. The inflammatory chemokines CCL2 and CCL5 in breast cancer. Cancer Letters. 2008; 267: 271–285.

[42] Yoshimura T, Robinson EA, Tanaka S, Appella E, Leonard EJ. Purification and amino acid analysis of two human monocyte chemoattractants produced by phytohemagglutinin-stimulated human blood mononuclear leukocytes. Journal of Immunology. 1989; 142: 1956–1962.

[43] Standiford TJ, Kunkel SL, Phan SH, Rollins BJ, Strieter RM. Alveolar macrophage-derived cytokines induce monocyte chemoattractant protein-1 expression from human pulmonary type II-like epithelial cells. The Journal of Biological Chemistry. 1991; 266: 9912–9918.

[44] Walker MJ, Barnett TC, McArthur JD, Cole JN, Gillen CM, Henningham A, *et al*. Disease manifestations and pathogenic mechanisms of Group A Streptococcus. Clinical Microbiology Reviews. 2014; 27: 264–301.

[45] Passos LSA, Jha PK, Becker-Greene D, Blaser MC, Romero D, Lupieri A, *et al*. Prothymosin Alpha: A Novel Contributor to Estradiol Receptor Alpha-Mediated $CD8^+$ T-Cell Pathogenic Responses and Recognition of Type 1 Collagen in Rheumatic Heart Valve Disease. Circulation. 2022; 145: 531–548.

[46] Haringman JJ, Gerlag DM, Smeets TJM, Baeten D, van den Bosch F, Bresnihan B, *et al*. A randomized controlled trial with an anti-CCL2 (anti-monocyte chemotactic protein 1) monoclonal antibody in patients with rheumatoid arthritis. Arthritis and Rheumatism. 2006; 54: 2387–2392.

[47] Miyabe Y, Lian J, Miyabe C, Luster AD. Chemokines in rheumatic diseases: pathogenic role and therapeutic implications. Nature Reviews. Rheumatology. 2019; 15: 731–746.

[48] Longobardi L, Temple JD, Tagliafierro L, Willcockson H, Esposito A, D'Onofrio N, *et al*. Role of the C-C chemokine receptor-2 in a murine model of injury-induced osteoarthritis. Osteoarthritis and Cartilage. 2017; 25: 914–925.

[49] Fantuzzi L, Tagliamonte M, Gauzzi MC, Lopalco L. Dual CCR5/CCR2 targeting: opportunities for the cure of complex disorders. Cellular and Molecular Life Sciences. 2019; 76: 4869–4886.